Deep-Sea Research II 55 (2008) 2352–2360

Contents lists available at ScienceDirect

Deep-Sea Research II

journal homepage: www.elsevier.com/locate/dsr2

Recent sediment accumulation rates for the Western margin of the Barents Sea

Agata Zaborska [a,*], JoLynn Carroll [b], Carlo Papucci [c], Leonardo Torricelli [c], Michael L. Carroll [b], Jolanta Walkusz-Miotk [a], Janusz Pempkowiak [a]

[a] Institute of Oceanology, Polish Academy of Sciences, Sopot, Poland
[b] Akvaplan-niva, Polar Environmental Center, 9296 Tromsø, Norway
[c] The Italian National Agency for New Technologies, Energy and the Environment, La Spezia, Italy

ARTICLE INFO

Available online 7 June 2008

Keywords:
Seafloor
Marginal ice zone
Sediment accumulation
Barents Sea

ABSTRACT

We investigate patterns, processes, and rates of sediment accumulation within the marginal ice zone of the western Barents Sea. The Barents Sea is among the most productive of the Arctic marginal seas, with approximately half of the sediment burial flux derived from marine rather than terrestrial sources. Sediment accumulation rates were quantified by ^{210}Pb geochronology at 14 stations, ranging in water depths from 173 to 503 m, along a south–north latitudinal gradient of 6° (75–81°N). The average sediment accumulation rate for all stations is 0.7 ± 0.4 mm/yr. In general, lower sediment accumulation rates are associated with coarser sediment fractions at shallower water depths (~200 m) where currents remove fine-grained sediments and transport material to the deeper regions. Higher sediment accumulation rates are detected in deeper water stations and are largely associated with specific sedimentation events and/or features of the Barents seafloor. Although the C/N ratio of surface sediments (0–2 cm) from all stations indicates a predominance of sediments of marine origin ($C/N = 9.0 \pm 1.0$), there is no distinct depositional pattern, indicating preferential burial in areas more heavily influenced by the marginal ice zone. We conclude that a combination of mixed sediment sources, large shifts in the location of the marginal ice zone over time, and the benthic boundary layer processes obscure the productivity signal preserved in these seafloor sediment deposits of the western Barents Sea.

1. Introduction

The vast majority (~70%) of sediment supplied to the Arctic Ocean accumulates in continental shelf seas. Among Arctic marginal seas, the Barents Sea is first in terms of total annual sediment burial, with an average burial rate of 259×10^6 t/yr, followed by the Kara Sea (194×10^6 t/yr), Beaufort Sea (123×10^6 t/yr), East Siberian Sea (109×10^6 t/yr), Laptev Sea (67×10^6 t/yr), and Chukchi Sea (19×10^6 t/yr), based on the sedimentary record for the Holocene era (0–11 kyr B.P.) (Stein and Macdonald, 2004). These sediment deposits consist of fine-grained clays and silts interspersed with layers of sand, representing typical marine, hemipelagic sedimentation (Ivanova et al., 2002). While the long-term sedimentary record for the Barents Sea has been well described through the analysis of seismic records, scant information exists on modern sediment accumulation processes and rates for this arctic marginal sea.

The Barents Sea is also the most productive of the Arctic seas, with a relatively high proportion (47%) of the sediment burial flux derived from marine rather than terrestrial sources (Stein and MacDonald, 2004). Sediments from bio-production are supplemented by terrestrial sources, namely rivers, coastal erosion, and aeolian transport. Although difficult to quantify, coastal erosion is probably the largest terrigenous sediment source, with recent estimates ranging from 59 (Rachold et al., 2004) to 119×10^6 t p yr (Stein and Macdonald, 2004). Barents Sea river inflow is small (163 km^3/yr) compared to other Siberian arctic shelf seas, with an associated sediment supply of only 18×10^6 t p yr (Holmes et al., 2002). The groundwater discharge sediment input is even lower, by an order of magnitude (Gordev et al., 1999). Compared to the other terrigenous sources, aeolian sediment input to the Barents Sea is negligible at 0.9×10^6 t p yr (Rachold et al., 2004).

Sea-ice sediment entrainment, transport, and melting processes have an influence on the re-distribution of Arctic sediments (Rachold et al., 2004; Dowdeswell et al., 1998). Sea ice has been shown to contain high amounts of inorganic material (Vinje and Kvambek, 1991), US quartz and clay minerals (Nürnberg et al., 1994) with biogenic components of only a few percent. Ice formed

* Corresponding author. Tel.: +48 585517283; fax: +48 585512130.
E-mail address: agata@iopan.gda.pl (A. Zaborska).

0967-0645/$ - see front matter © 2008 Elsevier Ltd. All rights reserved.
doi:10.1016/j.dsr2.2008.05.026

near the Yenisey and Ob rivers is transported by polar drift to the north Spitsbergen and northern Barents Sea area (Emery et al., 1997) reaching the Barents Sea within approximately 2 years (Eicken et al., 2005). Although the magnitude of this sediment source to the Barents Sea and elsewhere is still uncertain, Elverhøy et al. (1989) estimate that up to 30% of modern sedimentation in the Barents Sea may be connected to sea-ice/sediment interactions.

Sediments reaching the seafloor interact with bottom topography, resulting in areas of net deposition and erosion (Dowdeswell et al., 1998; Sternberg et al., 2001). Bottom topography in the Barents Sea is highly irregular, consisting of platform areas with depths of less than 200 m, basins and troughs with depths greater than 400 m. Deep troughs, located near Bear Island in Storfjorden and adjacent to Kvitøya exhibit complex morphological features that include glacial fans and seaward-convex-shaped bathymetries (Solheim et al., 1998). Turbidity currents are induced on the sloping sides of troughs where dense, downward-flowing waters create the potential for sediment transport from the shelf to the Arctic Ocean (Stein et al., 1994b; Sternberg et al., 2001; Dowdeswell et al., 1998). Shallow bank areas (100–200 m) consist of coarser sedimentary material due to strong tidal currents, while fine sediments are found along the eastern Svalbard coastline and in troughs (Elverhøi et al., 1989).

Quantification of modern rates of sediment accumulation aids in the interpretation of seafloor sediment biogeochemistry, e.g., nutrient cycling, organic carbon burial, sediment source identification, sediment reworking, and biodegradation (Carroll et al., 2008a; Renaud et al., 2008; Vandieken et al., 2006). The main objective of the present study is to increase the currently limited knowledge of the patterns, processes, and rates of modern seafloor sediment burial within the Barents Sea and in particular, in areas under the influence of the marginal ice zone. Rates derived in this study are based on the well-established ^{210}Pb geochronology approach, providing information on seabed processes operating over a time-scale of the order of 100 years.

2. Materials and methods

2.1. Field methods

Stations in the western Barents Sea are located along a general south to north latitudinal gradient of 6° (75–81°N) in (Fig. 1 and Table 1). Sediment cores were collected by multi-corer except for three stations where cores were sub-sampled from a box-corer (stations XII, XVII, XVIII). Sampling was performed in June 2003 (stations I, Ia, II, IIa, III, IV, Va), August 2004 (stations VIII, X, XI, XII) and May 2005 (stations XVI, XVII, XVIII). One sediment core from each cast was sub-sampled for ^{210}Pb (alpha spectrometry) and sediment properties into 1 cm intervals to 10 cm depth and 2-cm intervals until core bottom. Three other cores from the same cast were sub-sampled into 0.5-cm intervals to 5 cm depth and 1-cm intervals until 20 cm depth for the analysis of ^{137}Cs and ^{210}Pb by gamma spectrometry. Similar depth intervals were combined. All samples were dried at 60 °C and homogenized onboard the ship and stored in plastic bags until analyses.

2.2. Laboratory methods

2.2.1. Radiochemical procedures

One set of samples was transported to ENEA, La Spezia, Italy. Gamma-emitting radionuclides (^{210}Pb, ^{137}Cs) were measured using ORTEC high-purity planar germanium detectors. Detector efficiency was calibrated using several sources and verified using

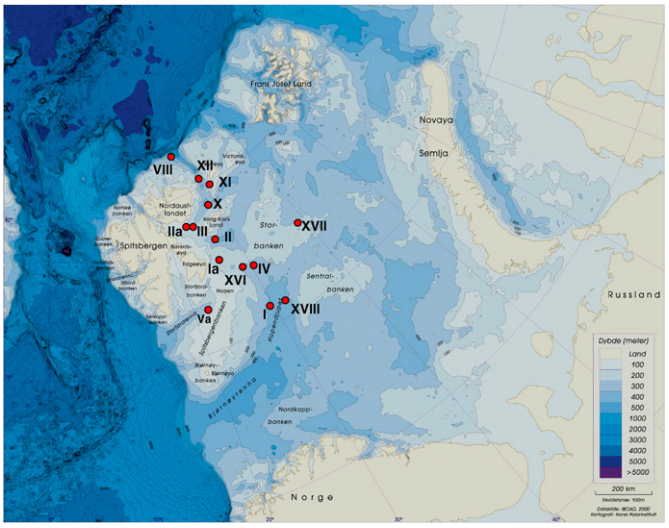

Fig. 1. Barents Sea bathymetry, bottom topography (Norwegian Polar Institute map) and benthic stations sampled during three cruises in 2003, 2004 and 2005.

an IAEA standard (IAEA-300). Detector blanks were determined from measurements performed on empty sample vials over a few days and these were found to be similar to natural background. Samples were stored in plastic containers for 21 days to allow for ingrowth of ^{214}Pb and ^{214}Bi prior to measuring ^{210}Pb. Total ^{210}Pb was determined by measurement of the 46.5 keV energy peak; $^{210}Pb_{supp}$ (^{226}Ra) was determined by measurement of ^{214}Pb (295 and 352 keV) and ^{214}Bi (609 keV). The $^{210}Pb_{ex}$ activity was determined by subtracting $^{210}Pb_{supp}$ (average of ^{214}Pb and ^{214}Bi activities) from total ^{210}Pb for each depth interval. Analyses were carried out on individual 20 g samples uniformly packed in vials of a standard geometry. Sediment activities were corrected for self-absorption (Cutshall et al., 1983). A second set of samples was transported to IOPAS, Poland where the daughter product of ^{210}Pb (^{210}Po) was quantified by alpha spectrometry. Analytical results derived by both alpha and gamma methods in this investigation were shown to be comparable (Zaborska et al., 2007) and thus ^{210}Po activities are not presented herein.

2.2.2. Sediment characterization

Grain size, porosity, density, and C_{org}/N_{tot} measurements were performed on individual depth layers from sediment cores. Samples for grain size analyses were transferred into Petri dishes, weighed and then transferred to a 60 °C oven for approximately two days to obtain stable sample dry weights. The dried samples were disaggregated and ground with an agate mortar and pestle. Porosity was determined using a wet–dry method [(water weight/dry sediment weight × 100]. Dry sediment density (g/cm^3) was derived according to the relation d_{sd} = (weight of dry sediment in the vial)/(volume of the dry sediment). Dry sediment volume was derived as the difference between the vial volume and volume of sediment water content (water volume = (weight of vial with undried sample–weight of vial with dried sample)/ density of seawater).

Grain size analyses were performed using a combination of dry sieving and electronic particle counting with a Sedigraph 5100. Samples were initially split into coarse (>0.063 mm) and fine (<0.063 mm) fractions by wet sieving, and then dried in 60 °C. The fraction above 0.063 mm was dry sieved for 15 min using sieves: 8, 4, 2, 1, 0.5, 0.25, 0.125 and 0.063 mm (Buchanan, 1984). The fine sediment fraction (below 0.063 mm) was suspended in 50 ml of distilled water, and sodium metaphosphate(V) was added. After placement in an ultrasound bath for 10 min, the

Table 1
Station location and water depth together with porosity, pelite fraction (<0.063 mm), radionuclide inventories and C_{org}/N_{tot} molar ratio in western Barents Sea sediments

Station	Latitude longitude	Location	Depth (m)	Porosity (0–20 cm)	Pelite fraction (%) (0–20 cm)	$^{210}Pb_{ex}$ inventory (Bq/cm^2)	^{137}Cs inventory (Bq/m^2)	C_{org}/N_{tot} mean ± st.dev. (range)
I	75°40′ 30°10′	Hopen Trench	345	0.86–0.70	77–93	0.27	40	8.3 ± 0.8 (7.0–9.7)
Ia	77°38′ 25°50′	Edgeøya	173	0.86–0.65		0.13		10.3 ± 1.6 (6.9–14.0)
II	78°15′ 27°10′	South Kong Karslandet	320	0.87–0.73	94–98	0.15	58	8.5 ± 1.5 (7.4–11.2)
IIa	70°03′ 25°37′	East Erik Eriksentretet	215	0.89–0.69		0.27		9.8 ± 1.4 (6.6–11.2)
III	79°01′ 25°46′	East Erik Eriksentretet	200	0.82–0.64	89–98	0.17	122	10.2 ± 1.4 (7.4–12.3)
IV	77°01′ 29°29	Hopen Bank	222	0.77–0.45	48–54	0.24	53	10.3 ± 2.4 (5.8–14.2)
Va	76°23′ 22°10′	Storfjordrenna	200	0.87–0.68		1.12		8.8 ± 1.6 (7.2–12.0)
VIII	81°17′ 26°51′	North Kvitøya Trench	503	0.82–0.70	94–98	1.19	142	
X	79°22′ 28°42′	North Kong Karsland	303	0.87–0.68	44–96	0.17	55	
XI	79°57′ 30°17′	North-East Kong Karsland	195	0.76–0.39	63–84	0.12	85	
XII	80°09′ 29°36′	Central Kvitøya Trench	286	0.85–0.66	86–95	0.28	81	
XVI	77°05′ 28°33′	North Hopen Deep	206	0.62–0.47	15–61	0.36	48	
XVII	77°26′ 40°18′	East Storbanken	208	0.84–0.63	78–83	0.09	30	
XVIII	75°41′ 31°49′	Hopen Trench	340	0.89–0.73	96–99	0.44	50	

sample was introduced to the Sedigraph. Grain size is given in weight percent of the total sample.

C_{org} and N_{tot} concentrations were determined for a limited number of samples. Carbonates were first removed by reaction with HCl, and then samples were rinsed in de-ionised water several times. Samples were dried, weighed and homogenized prior to measurement using a CHN Perkin-Elmer 2400 analyzer. The percentage of carbon was corrected for the weight change due to carbonate removal (Kristensen and Andersen, 1987). The inorganic fraction of nitrogen was assumed to be negligible because the organic carbon content is around 1%. Herein we refer to the ratio C_{org}/N_{tot}, as C/N.

2.2.3. ^{210}Pb accumulation rates and radionuclide inventories

Sediment accumulation rates are determined from profiles of excess ^{210}Pb activity ($^{210}Pb_{ex}$ = total ^{210}Pb-supported ^{210}Pb) versus porosity-corrected sediment depth. Sediment accumulation rates are calculated assuming an exponential decrease in $^{210}Pb_{ex}$ with sediment depth

$$A_t = A_0 e^{-\lambda x/v}$$

$$\ln\ ^{210}Pb_{ex}(x) = \ln\ ^{210}Pb_{ex}(0) - (\lambda/v)x$$

where $^{210}Pb_{ex}$ (x) is activity at layer x, $^{210}Pb_{ex}$ (0) is activity at layer 0, λ is the decay constant and v is the sediment accumulation rate (Robbins and Edgington, 1975). Rates were determined for three cases: assuming (a) no mixing, (b) mixing in first two sediment depth intervals, and (c) mixing in first four sediment depth intervals. For cases (b) and (c), sediment accumulation rates were quantified below the mixed layer. In all cases, the surface sediment (0 cm) $^{210}Pb_{ex}$ was allowed to vary to achieve a best-fit exponential profile based on a minimum least-squares fit criteria for the entire profile (surface to depth). The determined rates represent maximum rates as we do not consider mixing below the surface mixed zones designated in cases (b) and (c).

Inventories of $^{210}Pb_{ex}$ and ^{137}Cs were calculated as cumulative sum of $^{210}Pb_{ex}$ (Bq/g) and ^{137}Cs (Bq/g) multiplied by cumulative mass of each sediment layer (g/cm^2). $^{210}Pb_{ex}$ inventories are presented in Bq/cm^2 and ^{137}Cs inventories are given in Bq/m^2.

The statistical analysis program, *STATSTICA*, was used for the calculation of means, standard deviations, correlations and similarity between stations (Kruskal–Wallis test).

3. Results

3.1. Sediment characterization

Grain size analyses confirm that recent sediments are comprised of silty clays (Table 1), exhibiting a high pelite (grain size < 0.063 mm) content, low sand and gravel content. However a few stations contain a mixture of sediment types with a higher content of coarse sediments (stations IV and XVI) (Fig. 2). In general, coarser sediments are associated with shallow bank stations (~200 m depth). Among all stations, sediment porosities range from 0.62 to 0.89 in surface sediments (0–0.5 cm), decreasing with depth to 0.39–0.73 in layer 18–20 cm (Table 1).

C/N molar ratios for all sediment layers (0–20 cm) range from 5.8 to 14.2 (Table 1). C/N differs significantly among stations (Kruskal–Wallis test, $H = 24.9$, $P < 0.001$). Mean C/N ratios (0–20 cm) are highest at stations Ia, IIa, III, and IV (post hoc tests). Generally C/N is low (mean 9.0 ± 1.0) in the surface mixed layer (0–2 m) (Fig. 3) indicating a predominance of marine supplies. At most stations, C/N molar ratios do not decrease with depth (2–20 cm) due to organic matter mineralization and possibly to the impact of terrestrial sediment sources. In contrast, the C/N signature at station I (mean 8.4 ± 1.2) clearly reflects a predominance of marine organic matter supplies.

3.2. ^{210}Pb activities and radionuclide inventories

$^{210}Pb_{supp}$ values (^{210}Pb in equilibrium with the parent radionuclide, ^{226}Ra) ranged from a minimum of 27–28 Bq/kg (stations Va and XVI) to a maximum of 87 Bq/kg (station X). Stations in the central Barents Sea (I, IV, Va, XVI, XVII, XVIII) contain lower $^{210}Pb_{supp}$ values than northern stations (Ia, II, IIa, III, X, XI, XII, VII). $^{210}Pb_{supp}$ values are inversely correlated with sand and gravel content ($r^2 = 0.87$).

All $^{210}Pb_{ex}$ profiles decrease exponentially with depth until $^{210}Pb_{ex} = 0$, i.e. the $^{210}Pb_{supp}$ value is reached (Fig. 4). Two of the stations have very high surface $^{210}Pb_{ex}$ activities (VIII = 556 Bq/kg and XVIII = 724 Bq/kg). At station XVIII, sediment organic carbon content is also high (2.4%), which likely facilitated scavenging of ^{210}Pb to particles (He and Walling, 1996; Ab Razak et al., 1996). Station VIII, the northernmost station is located near the shelf break, an area under the influence of water masses moving onto and off the shelf. Relatively high $^{210}Pb_{ex}$ activities at this station are likely due to boundary scavenging (Huh et al., 1997;

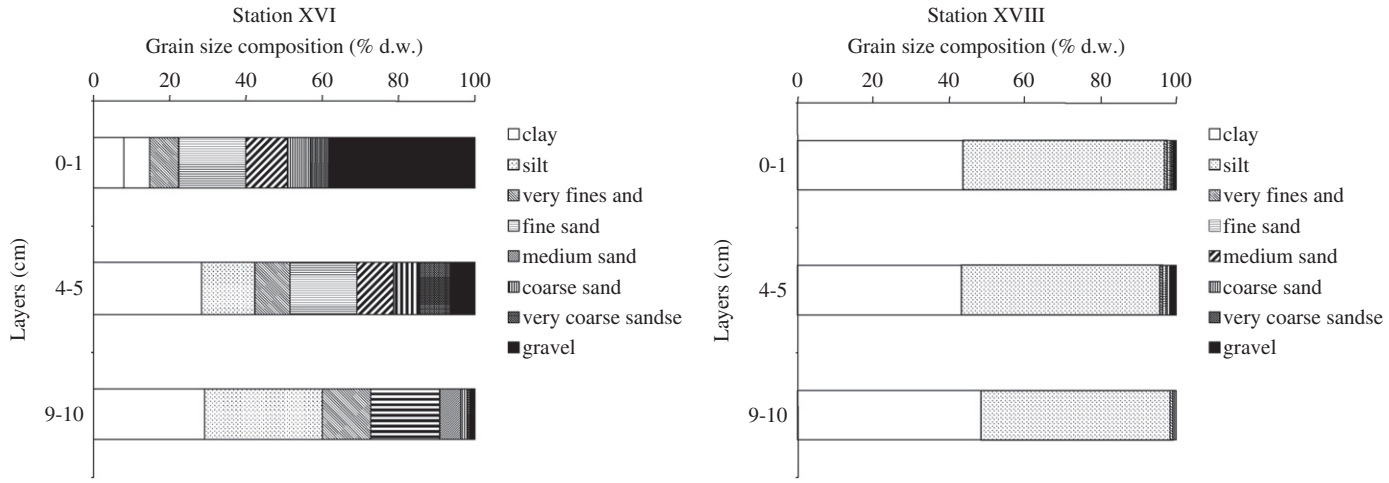

Fig. 2. Comparison of grain size composition at stations XVI and XVIII.

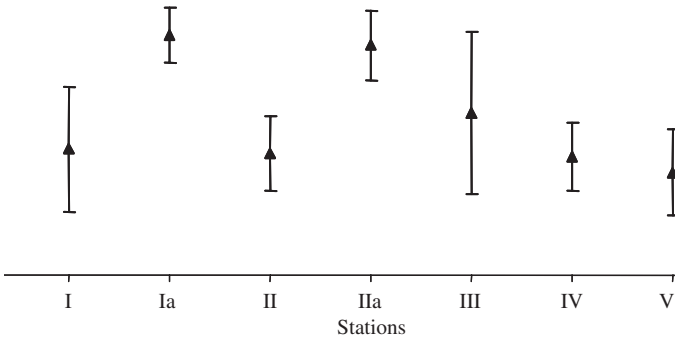

Fig. 3. Mean C/N ratio with standard deviation for surface (0–2 cm) sediment layers.

Smith et al., 2003). These sediments may also be resuspended repeatedly, allowing for additional absorption of ^{210}Pb from the water column (Smoak et al., 2000).

Inventories of $^{210}Pb_{ex}$ range from 0.09 up to 1.19 Bq/cm^2 (Table 1). The highest inventories are associated with stations VIII and Va, while the easternmost station, XVII, exhibits the lowest inventory. This station is located in the Storbanken–shallow bank area, where coarser sediments are observed. Stations Va and VIII exhibit both high sediment accumulation rates and $^{210}Pb_{ex}$ inventories.

^{137}Cs inventories are up to three times higher at stations VIII, XII, and III than at other stations (Table 1). Station III is located in Erik Eiksentretet between Nordauslandet and Kong Karls Land and may receive terrestrial material from coastal erosion or glaciers (Nordauslandet). Alternatively, terrestrial material may be derived from melting sea ice transported to this region. Stations VIII and XII are part of the Kvitøya Trench system, which extends from the shelf into the Arctic Ocean. ^{137}Cs signatures in sediments at these two locations may be influenced by water masses originating in the Arctic Ocean.

3.3. Sediment accumulation rates

Both physical and biological mixing confounds sediment burial histories through post-depositional alterations in the $^{210}Pb_{ex}$ activity depth profile. Hence sediment accumulation must be evaluated in combination with sediment mixing (Robbins, 1978; Berner, 1980; Boudreau, 1986). Visual evidence of surface mixing is evident in $^{210}Pb_{ex}$ profiles for stations I, IV, Va, and VIII (Fig. 4). To account for the influence of surface sediment mixing on all $^{210}Pb_{ex}$ sediment profiles, we evaluate the sensitivity of rate determinations assuming different surface mixed depths (0, 2, and 4 depth intervals). At nearly all stations, accumulation rates for the three different test cases are within 10% of the average; stations IV, Va, X, and XI are within 20% of their average rates (Fig. 5). These rates represent upper limit values for sediment accumulation because the approach assumes no mixing is occurring below the upper four depth intervals ($\leqslant$3 cm). Carroll et al. (2008a), also apply a formalized two layer mixing model to evaluate the influence of mixing on each profile. Their determined ^{210}Pb mixing rates were typically from 0.03 to 0.1 cm^2/yr.

Very low sediment accumulation rates (0.2–0.4 mm/yr) were determined at stations IV, XI, XII, and XVI (Fig. 5). At stations I, Ia, II, IIa, III, X, and XVII accumulation rates were higher (0.5–0.7 mm/yr). The highest accumulation rates (0.9–1.3 mm/yr) were measured at stations Va, VIII, and XVIII. In general, sediment accumulation rates are higher (e.g., VIII and XVIII) at stations with the highest average pelite fraction ($\geqslant$97%) while stations with coarse material (e.g., IV and XVI), and average pelite fractions ($\geqslant$60%) exhibit low accumulation rates (0.2 mm/yr). Both stations VIII and Va are located in underwater trench systems, where sediments supplied from the surrounding slopes may be transported through sediment focussing to these locations.

^{137}Cs is often used as an independent check on sediment accumulation rates by ^{210}Pb (Carroll and Lerche, 2003). In the Barents Sea data set, peaks in ^{137}Cs activity connected to human activities (i.e. Chernobyl accident, peak period of atmospheric nuclear weapons testing) are not clearly recognizable in sediments because of generally low radionuclide activities (see ^{137}Cs inventories given in Table 1). If we calculate sediment accumulation rates by assigning an age of 1950 to the deepest depth of ^{137}Cs penetration, the determined ^{137}Cs accumulation rates are slightly higher than those determined from the $^{210}Pb_{ex}$ profiles. Given the greater degree of uncertainty in the ^{137}Cs estimates, the ^{137}Cs results generally support our ^{210}Pb dating results.

4. Discussion

^{210}Pb sediment accumulation rates derived for the western Barents Sea integrate variations in water masses, ice cover, productivity regimes, and sediment sources operating over 10's

to 100 years. We have quantified rates at a number of sites along a north–south transect to provide baseline information on modern depositional regimes in this poorly investigated region. Based on future climate scenarios, significant changes in sediment sources are likely for this arctic marginal sea as a result of changes in sea ice distributions, freshwater inflow, and marine productivity. Thus it is critical to derive quantitative information as a baseline for future comparisons. Accumulation rates, based on the assumption of mixing confined to a shallow surface layer, represent upper limit rate estimates for the region; also see Carroll et al. (2008a). These rate determinations support the interpretation of results from other investigators

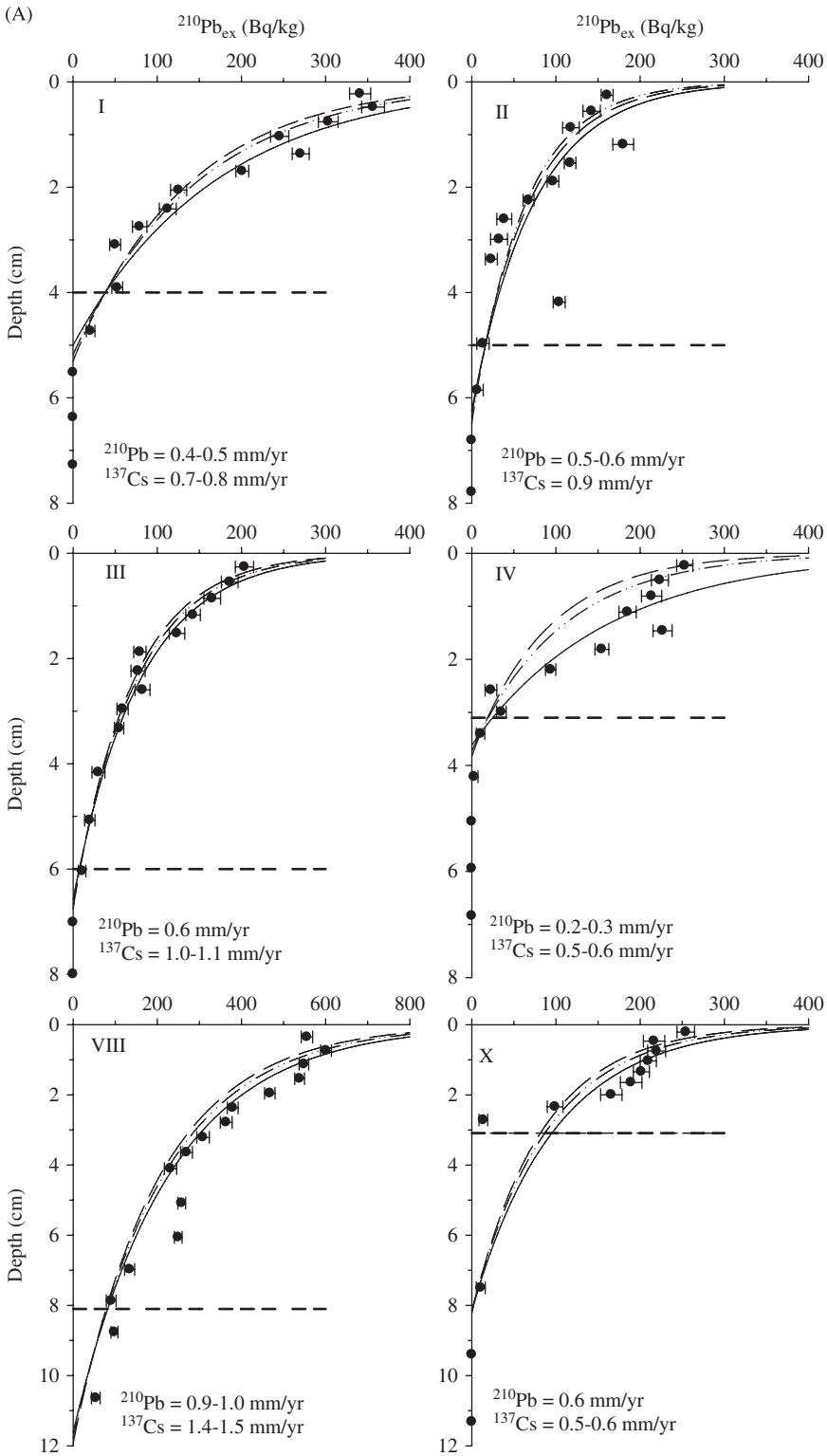

Fig. 4. $^{210}Pb_{ex}$ depth profiles for all stations. Sediment accumulation rates were determined for three cases: (A) no mixing (solid line), (B) mixing in upper 2-depth intervals (dash-dot-dot), (C) mixing in upper 4-depth intervals (dashed line). Heavy dashed horizontal line indicates the depth of ^{137}Cs penetration.

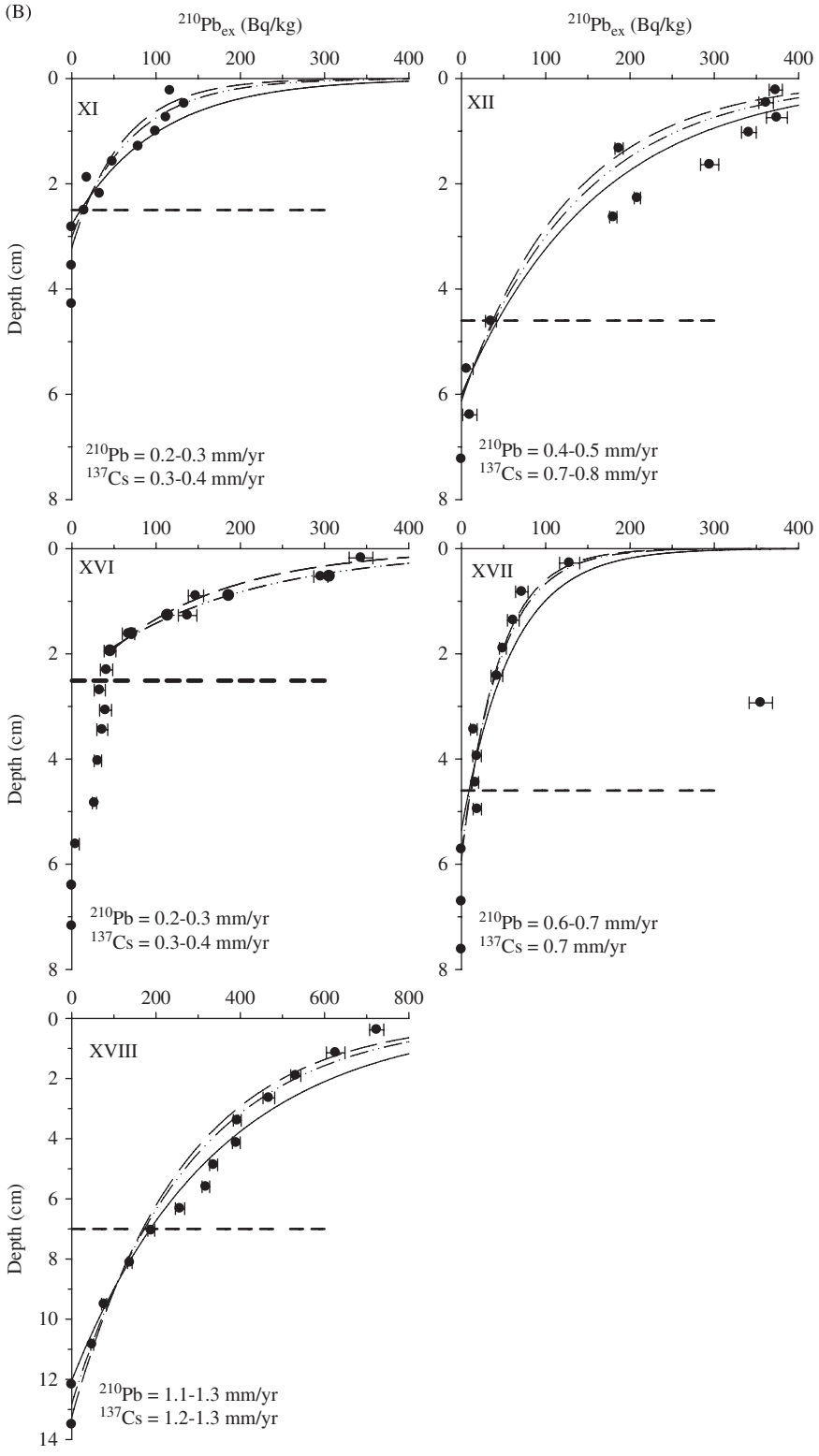

Fig. 4. (*Continued*)

under the multi-disciplinary CABANERA framework (Wassmann et al., 2008).

Maximum sediment accumulation rates quantified below the mixed depth (0–3 cm) are generally low, throughout the region, ranging from 0.2 to 0.8 mm/yr at most stations. Higher rates (0.9–1.3 mm/yr) are observed at stations Va (Storfjorden Trench), VIII (Kvitøya Trench) and XVIII (Hopen Trench), as well as station X (North Kong Karlsland). These rates are comparable to rates determined for the eastern Barents Sea which ranged from 0.0 to 1.6 mm/yr (Smith et al., 1995) but lower than nearshore stations in both the eastern Barents Sea (Smith et al., 1995) and fjords of Svalbard (Hald et al., 2001).

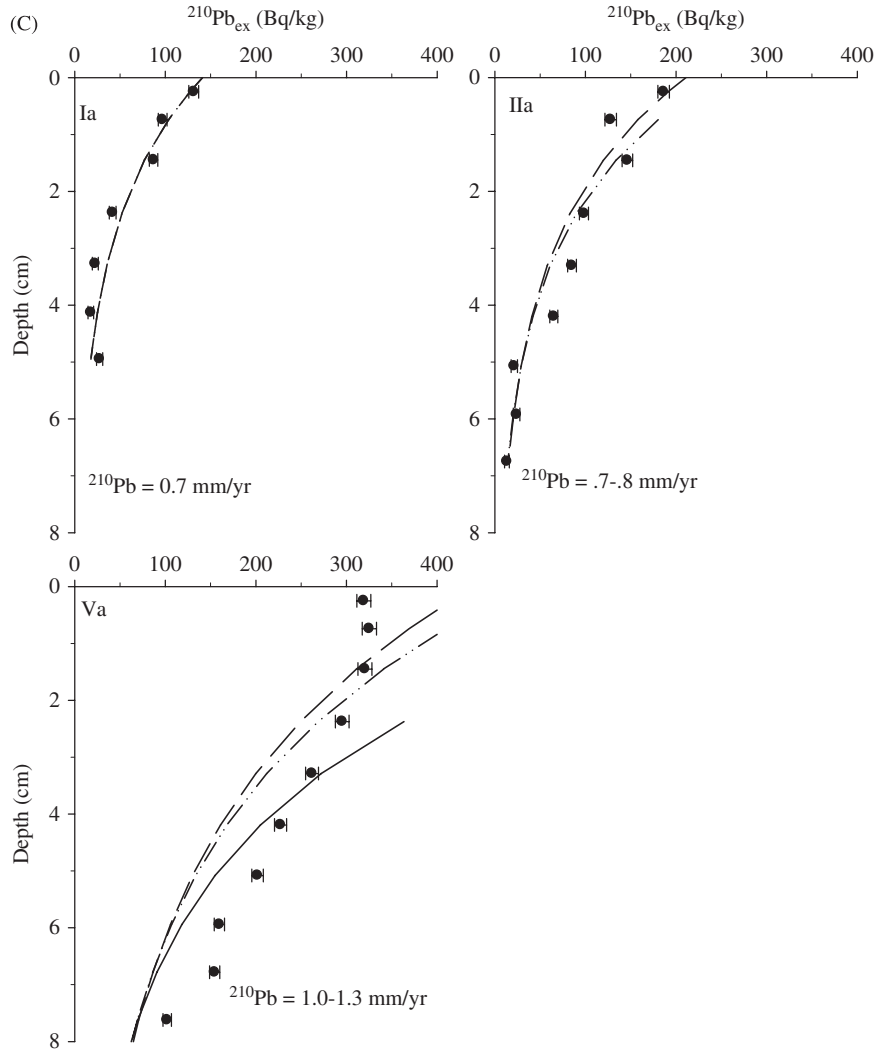

Fig. 4. (*Continued*)

The relative proportion of particulate matter supplied by bioproduction versus terrigenous sources is highest in the Barents Sea compared to other arctic marginal seas (Stein and MacDonald, 2004). Seafloor sediments in the western Barents Sea reflect this, consisting in most places of mixed sources based on C/N ratios which vary from 5.8 to 14.2. Coarse sediments ($50.9 \pm 3.6\%$ of >0.063 mm grain-size fraction), a visible mixed layer and low-sediment accumulation rate, are found at Hopen Bank (station IV). At this location strong (27 cm/s) bottom currents were previously reported (Sternberg et al., 2001). These conditions are not conducive to the preservation of organic matter, thus the observed higher C/N below the surface mixed layer may be connected to terrestrial material transported by bottom currents. In contrast, sediments deposited in Hopen Trench (station I) are mainly of marine origin.

^{137}Cs is mainly supplied by terrestrial sources rather than as a result of scavenging from the water column (Baskaran et al., 1996). High ^{137}Cs inventories at stations III and VIII probably result from a higher proportion of terrigenous supplies from coastal erosion, glaciers, or sea-ice melt in the vicinity of Svalbard. This is supported by a high C/N ratio at station III.

Within the deep Kvitøya trench (station VIII) we find a distinctly higher radionuclide inventory that likely result from the greater influence of Arctic Ocean waters moving onto the shelf through this passageway. Here too, the sediment accumulation rate is exceptionally high, probably as a consequence of sediment focussing related to the relatively steep depth gradients found in this region of the shelf (Vandieken et al., 2006; Carroll et al., 2008a, b). Station XVIII in Hopen trench, is a deep depression in the southern Barents Sea, consisting of fine-grained, high porosity sediments, primarily of marine origin (Carroll et al., 2008a, b; Reigstad et al., 2008). Rather than sediment focussing, water-column particle flux processes appear to dominate at this station; a mechanism observed during the time of sampling when passage of a storm resulted in a fully mixed water column and a pulse of particulate matter enriched in $^{234}Th_{ex}$ to the seafloor (Carroll et al., 2008a). At this station, $^{234}Th_{ex}$ was detected down to 1.5 cm below the sediment surface.

In contrast, shallow bank areas (100–200 m) exhibit coarser sediments and we document generally low–sediment accumulation rates (e.g., stations IV and XVI) in these areas. One exception is station X, but the profile at this station does not exhibit a smooth exponential decrease in $^{210}Pb_{ex}$ with sediment depth resulting in a less reliable accumulation rate. In general, we expect that most shallow bank areas are exposed to strong near-bed current velocities and bottom stresses which periodically exceed the threshold of grain motion. This results in sediment re-suspension events that lessen the potential for sediment burial.

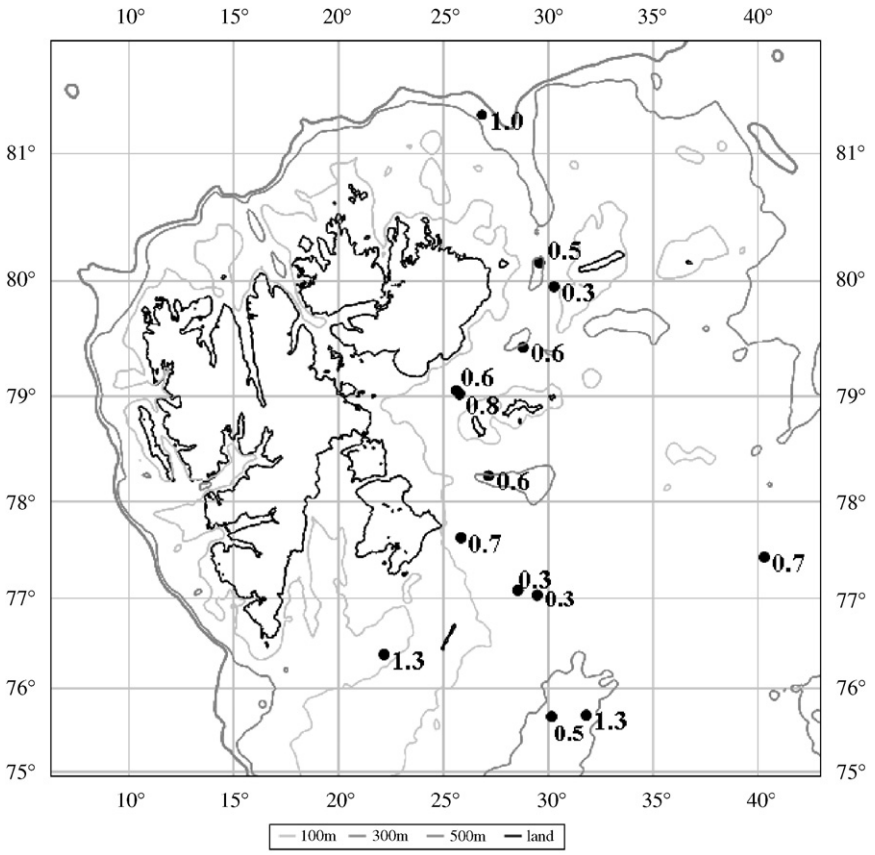

Fig. 5. ^{210}Pb sediment accumulation rates in mm/year (maximum rates, without mixing).

These conditions have been documented and described previously by Sternberg et al. (2001) for the shallow banks surrounding Storfjordrenna and in the region between Edgeøya and Kong Karls Land, in water depths up to 200 m.

No distinct depositional pattern emerges in our sediment accumulation rates to indicate the preferential burial in areas more heavily influenced by productivity patterns associated with the marginal ice zone (Wassmann et al., 2006). The combination of mixed sediment sources, large shifts in the location of the marginal ice zone over time and benthic boundary layer controls on seafloor sediment dynamics override this signal. Depth alone, also does not correlate with sediment accumulation rate. As expected we do observe a positive trend between sediment accumulation rate and grain size with higher rates at stations with the highest average pelite fraction (e.g., VIII, XVIII$\geqslant$97%) and low accumulation rates (0.2 mm/yr) at stations with lower average pelite fractions (e.g., IV, XVI$\geqslant$60%).

5. Conclusions

Among all stations evaluated within this study, the average sediment accumulation rate is 0.7 ± 0.4 mm/yr. The derived ^{210}Pb based sediment accumulation rates represent the integration of physical and biological processes operating in the northwest Barents Sea over decadal and longer time scales. Despite relatively similar accumulation rates (0.2–0.8 mm/yr) at most stations, different depositional conditions and sedimentary sources dominate among stations, as seen from radionuclide concentrations, inventories and C/N ratios. These sources include sediment supplies of terrigeonous material from Svalbard and/or sea ice and marine productivity. Generally, lower sediment accumulation rates are associated with shallow depths (~200 m) while burial rates at deeper stations are largely associated with specific events and/or features of the Barents seafloor.

Acknowledgments

We acknowledge the captain and crew of R/V *Jan Mayen* for their support and assistance at sea during the CABANERA project, "Carbon flux and ecosystem feedback in the northern Barents Sea in an era of climate change". O. Isaksen provided essential logistical support for the benthos group. Special thanks to the laboratory personnel at both ENEA and IOPAS who assisted in all phases of the analytical work. We thank Agata Sørflaten for assistance in the modelling of the tracer profiles. Roberta Delfanti contributed valuable advice and support, particularly during A. Zaborska's ENEA internships. Our thanks to Paul Wassmann and the members of the CABANERA project for sharing their ideas and data. Finally, we wish to thank the Norwegian Research Council Project for financial support to CABANERA (project number: 155936/700) with additional financial support provided by the Polish State Committee for Scientific Research (Grant no. 2PO4E 007 28), Institute of Oceanology Poland, The Italian National Agency for New Technologies, Energy and the Environment, and Akvaplan-niva.

References

Ab Razak, I.A., Li, A., Christensen, E.R., 1996. Association of PAHs, PCBs, Cs-137 and Pb-210 with clay, silt and organic carbon in sediments. Water Science and Technology 34 (7–8), 29–35.

Berner, R., 1980. Early Diagenesis—A Theoretical Approach. Princeton University Press, Princeton, NJ, p. 241.
Boudreau, B.P., 1986. Mathematics of tracer mixing in sediments. I: spatially-dependent, diffusive mixing. II: Non local mixing and biological conveyor-belt phenomena. American Journal of Science 286, 161–238.
Buchanan, J.B., 1984. Sediment analysis. In: Holme, N.A., McIntyre, A.D. (Eds.), Methods for the Study of Marine Benthos. Blackwell Scientific Publishers, Boston.
Carroll, J., Lerche, I., 2003. Sedimentary Processes: Quantification Using Radionuclides. Elsevier, p. 272.
Carroll, J., Zaborska, A., Papucci, C., Schirone, A., Carroll, M., Pempkowiak, J., 2008a. Accumulation of organic carbon in western Barents Sea sediments. Deep-Sea Research II, this issue [doi:10.1016/j.dsr2.2008.05.005].
Carroll, M.L., Denisenko, S., Renaud, P., Ambrose, W., 2008b. Benthic infauna of the seasonally ice-covered Western Barents Sea: patterns and relationships to environmental forcing. Deep Sea Research II, this issue [doi:10.1016/j.dsr2.2008.05.022].
Cutshall, N.H., Larsen, I.L., Olsen, R., 1983. Direct analysis of ^{210}Pb in sediment samples: self absorption corrections. Nuclear Instruments and Methods 206, 309–312.
Dowdeswell, J.A., Elverhøi, A., Spielhagen, R., 1998. Glaciomarine sedimentary processes and facies on the polar north Atlantic margins. Quaternary Science Reviews 17, 243–272.
Emery, W.J., Fowler, C., Maslanik, J., Pfirman, S., 1997. New satellite derived sea ice motion tracks Arctic contamination. Marine Pollution Bulletin 35, 345–352.
Eicken, H., Gradinger, R., Gaylord, A., Mahoney, A., Rigor, I., Melling, H., 2005. Sediment transport by sea ice in the Chukchi and Beaufort seas: increasing importance due to changing ice conditions? Deep-Sea Research II 52, 3281–3302.
Elverhøi, A., Phirman, S.L., Solheim, A., Larssen, B.B., 1989. Glaciomarine sedimentation in epicontitental seas exemplified by the northern Barents Sea. Marine Geology 85, 225–250.
Gordev, V.V., Dzhamalow, R.G., Zektser, I.S., Zhulidov, A.V., Brysgalo, V.N., 1999. An assessment of groundwater input of nutrients into the coastal seas the Rusian Arctic. Water Resources 38, 1–6.
Hald, M., Dahlgren, T., Olsen, T.-E., Lebesbye, E., 2001. Late Holocene palaeoceanography in Van Mijenfjorden, Svalard. Polar Research 20 (1), 23–35.
He, Q., Walling, D.E., 1996. Interpreting particle size effects in the adsorption of Cs-137 and unsupported Pb-210 by mineral soils and sediments. Journal of Environmental Radioactivity 30 (2), 117–137.
Holmes, M.R., McClelland, J.W., Peterson, B.J., Shiklomanov, I.A., Shiklomanov, A.I., Zhulidov, A.V., Gordeev, V.V., Bobrovitskaya, N.N., 2002. A circumpolar perspective of fluvial sediment flux to the Arctic Ocean. Global Biogeochemical Cycles 16, 4–10.
Huh, C., Pisias, N.G., Kelley, J.M., Maiti, T.C., Grantz, A., 1997. Natural radionuclides and plutonium in sediments from the western Arctic Ocean: sedimentation rates and pathways of radionuclides. Deep-sea Research II 44 (8), 1725–1743.
Ivanova, E.V., Murdmaa, I.O., Duplessy, J.C., Paterne, M., 2002. Late Weichselian to Holocene paleoenvironments in the Barents Sea. Global and Planetary Change 34, 209–218.
Kristensen, E., Andersen, F.Ø., 1987. Determination of organic carbon in marine sediments: a comparison of two CHN-analyzer methods. Journal of Experimental Marine Biology and Ecology 109, 15–23.
Nürnberg, D., Wollenburg, I., Dethleff, D., Eicken, H., Kassens, H., Letzig, T., Reimnitz, E., Thiede, J., 1994. Sediments in Arctic sea ice: implications for entrainment transport and release. Marine Geology 119, 185–214.
Rachold, V., Eicken, H., Gordeev, V.V., Grigoriev, M.N., Hubberten, H.-W., Lisitzin, A.P., Shevchenko, V.P., Schirrmeister, L., 2004. Modern terrigenous organic carbon input to the Arctic Ocean. In: Stein, R., Macdonald, R.W. (Eds.), The Organic Carbon Cycle in the Arctic Ocean. Springer, Berlin, Heidelberg, pp. 315–322.
Reigstad, M., Wexels-Riser, C., Wassmann, P., Ratkova, T., 2008. Vertical export of particulate organic carbon: attenuation, composition, and loss rates in the Northern Barents Sea. Deep-Sea Research II, this issue [doi:10.1016/j.dsr2.2008.05.007].
Renaud, P.E., Morata, N., Carroll, M.L., Denisenko, S.G., Reigstad, M., 2008. Pelagic–benthic coupling in the Western Barents Sea: processes and time scales. Deep-Sea Research II, this issue [doi:10.1016/j.dsr2.2008.05.017].
Robbins, J.A., 1978. Geochemical and geophysical applications of radioactive lead. In: Nriagu, J.O. (Ed.), The Biogeochemistry of Lead in the Environment. Elsevier, pp. 285–393.
Robbins, A., Edgington, D.N., 1975. Determination of recent sedimentation rates in Lake Michigan using Pb-210 and Cs-137. Geochimica et Cosmochimica Acta 39, 285–304.
Smith, J.N., Ellis, K.M., Naes, K., Dahle, S., Matishov, D., 1995. Sedimentation and mixing rates in the Barents Sea sediments off Novaya Zemlya. Deep-Sea Research II 42, 1471–1493.
Smith, J.N., Moran, S.B., Macdonald, R.W., 2003. Shelf-basin interactions in the Arctic Ocean based on ^{210}Pb and Ra isotope tracer distributions. Deep-Sea Research I 50, 397–416.
Smoak, J.M., Moore, W.S., Thunell, R.C., 2000. Influence of boundary scavenging and sediment focusing on ^{234}Th, ^{228}Th and ^{210}Pb fluxes in the Santa Barbara Basin. Estuarine, Coastal and Shelf Science 51, 373–384.
Solheim, A., Faleide, J.I., Andersen, E.S., Elverhøi, A., Forsberg, C.F., Vanneste, K., Uenzelmann-Neben, G., Channell, J.E.T., 1998. Late Cenozoic seismic stratygraphy and glacial geological development of the East Greenland and Svalbard-Barents Sea continental margins. Quaternary Science Reviews 17, 155–184.
Stein, R., Macdonald, R.W., 2004. Organic carbon budget: Arctic vs. global ocean. In: Stein, R., Macdonald, R.W. (Eds.), The Organic Carbon Cycle in the Arctic Ocean. Springer, Berlin, Heidelberg, pp. 315–322.
Stein, R., Grobe, H., Wahsner, M., 1994b. Organic carbon, carbonate, and clay mineral distributions in eastern central Arctic Ocean surface sediments. Marine Geology 119, 269–285.
Sternberg, R.W., Aagaard, K., Cacchione, D., Wheatcroft, R.A., Beach, R.A., Roach, A.T., Marsden, M.A.H., 2001. Long-term near-bed observations of velocity and hydrographic properties in the northwest Barents Sea with implications for sediment transport. Continental Shelf Research 21, 509–529.
Wassmann, P., Reigstad, M., Haug, T., Rudels, B., Carroll, M.L., Hop, H., Gabrielsen, G.W., Falk-Petersen, S., Denisenko, S.G., Arashkevich, E., Slagstad, D., Pavlova, O., 2006. Food webs and carbon flux in the Barents Sea. Progress in Oceanography 71 (2–4), 232–287.
Vandieken, V., Nickel, M., Jørgensen, B.B., 2006. Carbon mineralization in Arctic sediments northeast of Svalbard: Mn(IV) and Fe(III) reduction as principal anaerobic respiratory pathways. Marine Ecology Progress Series 322, 15–27.
Vinje, T., Kvambek, Å.S., 1991. Barents Sea drift ice characteristics. Polar Research 10, 59–68.
Zaborska, A., Carroll, J., Papucci, C., Pempkowiak, J., 2007. Intercomparison of alpha and gamma spectrometry techniques used in ^{210}Pb geochronology. Journal of Environmental Radioactivity 93, 38–50.